

Feature-size reduction of photopolymerized structures by femtosecond optical curing of SU-8

Kock Khuen Seet, Saulius Juodkazis,^{a)} Vygandas Jarutis, and Hiroaki Misawa^{b)}
 CREST-JST, Research Institute for Electronic Science, Hokkaido University, N21W10 CRIS Building,
 Sapporo 001-0021, Japan

(Received 7 March 2006; accepted 22 May 2006; published online 13 July 2006)

The universal scaling of a width of photopolymerized line on the exposure dose was observed in polymerization by direct laser writing using tightly focused femtosecond pulses in SU-8 resist. This scaling can be explained as the photopolymerization by a blackbody-type emission. A spectrally broad thermal emission of electrons heated up to temperatures approximately $T_e \sim 10^3$ K coincides with an IR-absorption band of SU-8 centered at the $2.9 \mu\text{m}$ and had caused polymerization by a cumulative direct absorption. Three-dimensional photonic crystal templates with approximately twice reduced feature size were fabricated with stop band at the fiber communication wavelength of $1.3 \mu\text{m}$. © 2006 American Institute of Physics. [DOI: 10.1063/1.2221499]

The light intensity up to few TW/cm^2 can be delivered inside materials when subpicosecond laser pulses of tens of nanojoules are focused into a spot size of subwavelength cross sections transferring solid matter into plasma via multiphoton and avalanche ionization.^{1,2} Such three-dimensionally enclosed ionized volume creates a high-pressure and high-temperature region where phase transitions and new materials are expected to be formed^{3,4} and could be patterned with a submicrometer resolution.⁵ Here, we demonstrate how a 3D localized ionization of resist alters a usual photopolymerization of an UV-curable resist at high irradiance. It is shown that thermal emission of hot nonequibrated electrons $T_e \sim 10^3$ K accounts for polymerization of resist when femtosecond tightly focused nanojoule pulses are used for direct laser writing. A universal scaling of the width of polymerized rod on the exposure dose has been established.

The UV-curable SU-8 resist has become a popular recording material in microelectromechanical system^{6,7} (MEMS) and micropotonics⁸ due to its high structural strength and chemical resistivity. Recently SU-8 has become widely utilized as a template material for photonic crystal applications.^{8,9} The femtosecond near-IR direct laser writing⁹ or holographic recording¹⁰ is used to form three-dimensional (3D) patterns in SU-8. The UV photopolymerization of SU-8 proceeds via a cationic mechanism^{7,11} via diffusion on a time scale longer than 1 ms.¹² In the case of near-IR femtosecond pulses, the photoinitiation step of SU-8 polymerization starts via nonlinear, usually, two-photon absorption.¹³ For practical applications, it is necessary to establish which irradiance and overlap between exposed regions, at which pulse energy (maintaining the same exposure dose), would yield in structurally most robust patterns and would achieve the smallest feature size.¹⁴

We have recorded 3D suspended rods with different separation between exposed regions, Δ , by direct laser writing at different pulse energies in negative resist SU-8 [Fig. 1(a)] using an 800 nm wavelength and 180 fs radiation. The

rods were tilted and embedded into a supporting structure, as shown in Fig. 1(b). Such method allowed to avoid focal volume alterations by an interface between substrate (cover glass) and SU-8 film and to form 3D suspended rods after development. The lateral cross section of the rods [Fig. 1(c)] was determined by the scanning electron microscopy (SEM). When Δ was made of the same order as the rod's lateral cross section, the individual voxels became apparent as a chain of connected beads (not shown). For a small Δ quality of rods deteriorates at higher pulse energy [Fig. 2(b)] due to optical breakdown (a full ionization of focal volume). Interestingly, there exist conditions where rods can be fabricated without a standard postexposure bake. It was found that without postbake, the lateral and axial dimensions were typically twice smaller [Figs. 2(c) and 2(d)] as compared with those obtained by standard protocol [Figs. 2(a) and 2(b)]. It is noteworthy that the postexposure is considered a compulsory step¹⁵ since the exposure alone is not providing necessary cross-linking and polymerization even for UV exposure. This observation hinted that the annealing took place during direct laser writing.

To establish the mechanism behind the apparently thermal polymerization of SU-8 by ultrashort pulses, the rods were recorded and processed by a standard protocol [Fig. 1(c)]. The diameter of the rod at its suspended part was measured as function of pulse energy E_p and pitch Δ . These data are summarized in Fig. 3(a). It was found that a particular scaling exists, namely, all experimental data obeyed the same dependence [Fig. 3(b)]:

$$d = w_0 \sqrt{2 \ln(g^{1/4} E_p / E_{\text{th}})}, \quad (1)$$

where the factor g reflects geometrical overlap of subsequent Gaussian pulses and was estimated as

$$g = \sum_{n=-\infty}^{\infty} e^{-2(n\Delta)^2/w^2} = 1 + 2 \sum_{n=1}^{\infty} e^{-2(n\Delta)^2/w^2}, \quad (2)$$

where Δ is the pitch between adjacent pulses and w is the focal diameter. The factor g approach 1 for $\Delta/w \gg 1$ and has approximate value of $(\pi/2)^{1/2} w/\Delta$ for $\Delta/w \ll 1$. All experimental data obeyed the same dependence [Eq. (1)], which can be interpreted as a polymerization yield: the lateral di-

^{a)}Electronic mail: saulius@es.hokudai.ac.jp

^{b)}Author to whom correspondence should be addressed; electronic mail: Misawa@es.hokudai.ac.jp

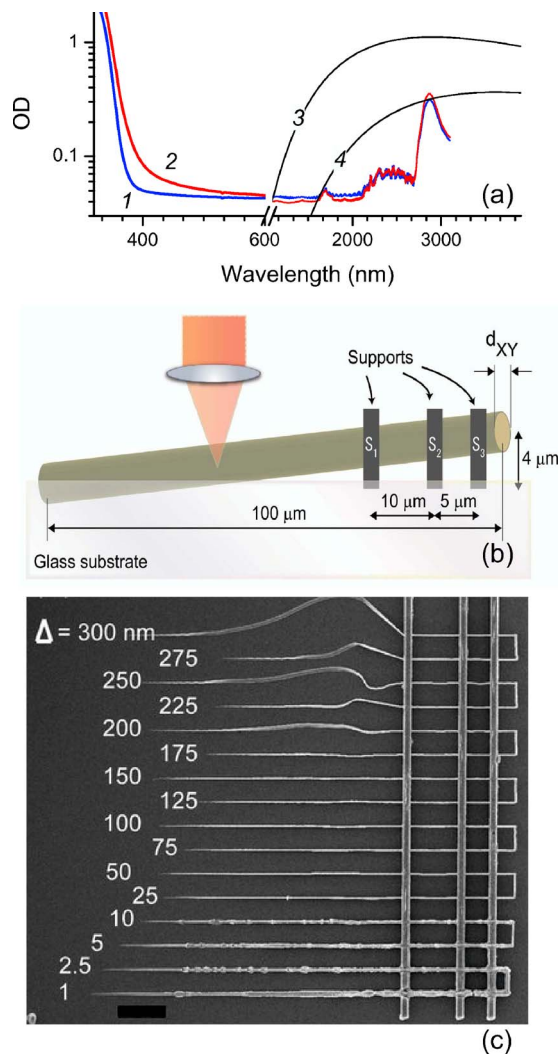


FIG. 1. (a) Absorption spectrum of an as-coated SU-8 film (1) and after full UV polymerization (2). The spectral profiles of blackbody radiation at 1000 K (3) and 800 K (4) are shown. (b) Schematics of the 3D suspended rods' recording. (c) SEM image of pattern recorded at $E_p=0.868$ nJ at different intrapulse separation Δ . Scale bar, 10 μm .

iameter of the polymerized rod d plotted versus the product of the pulse energy E_p and temperature T , assuming $T \sim \sqrt[4]{g}$. Justification of this assumption is discussed below.

Thermal emission of hot electrons during the pulse and immediately after it, before thermal equilibration with ions and atoms, should be considered as a possible source of a blackbody-type radiation with a considerable IR spectral component, which can enhance polymerization of SU-8 by direct absorption in a 2–3 μm spectral region [Fig. 1(a)]. The electron temperature of $T_e \sim 1000$ K (relevant to our irradiation conditions as shown below) has the maximum emission in the IR vibrational spectral region of SU-8 absorption [Fig. 1(a)]. The Stephan-Boltzmann law for a stationary emitted energy density sets thermal dependence as $\propto T^4$. The multipulse exposure (at small Δ) has caused a cumulative effect on polymerization (Fig. 3) via cumulative absorption of the blackbody radiation [as given by Eq. (1)]. The required exposure was accumulated via multipulse irradiation at smaller pulse energy. Since the pulse duration is much shorter than the thermal diffusion time, the instantaneous electron temperature profile is assumed to repeat the pulse profile, i.e., $T_e(r) \propto I(r)$ while the ions/atoms are not

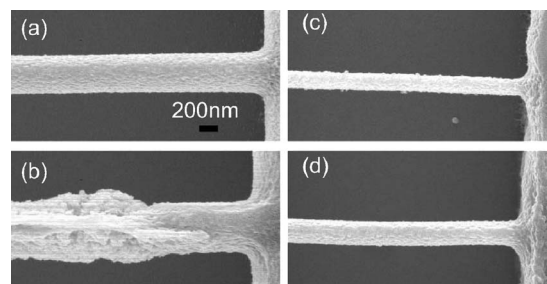


FIG. 2. SEM images of rods recorded by the standard procedure [(a) and (b)] and without the postbake [(c) and (d)] at $E_p=0.52$ nJ, $\Delta=10$ nm [(a) and (c)] and 0.608 nJ, 5 nm [(b) and (d)], respectively.

heated during the pulse. Since the pulse intensity is proportional to its energy, we define the threshold condition for polymerization (which results in solid voxels) as

$$g(E_p e^{-2x^2/w^2})^4 = E_{\text{th}}^4. \quad (3)$$

This simple model provides the correct voxel's diameter dependence on exposure dose [Eq. (1)] with the same E_{th} value. Hence, the polymerization can be explained by the cumulative direct absorption of blackbody emission of hot electrons.

Let us make a qualitative estimate for the electron temperature T_e during recording, since the T_e value defines the effective spectral width of the blackbody radiation. The quiver energy of electrons $\epsilon_{\text{osc}} \approx 9.4 I \lambda^2$ (in [eV]), where I is the laser irradiance in 10^{14} W/cm² and the wavelength λ is in micrometers. The irradiance per single 0.5 nJ, $t_p = 180$ fs, $\lambda = 800$ nm pulse is $I = 2$ TW/cm² calculated at a full width at half maximum (FWHM) of intensity envelope. The waist, radius, of the focal spot was estimated as a radius of Airy disk $w_0 = 0.61 \lambda / \text{NA}$ at a $1/e^{-2}$ level, where $\text{NA} = 1.35$ is the numerical aperture of objective lens. The factor of $\sqrt{\ln 2/2}$ was used to recalculate the waist at the FWHM level assuming a Gaussian intensity profile. At such irradiance the rate of electron generation by avalanche is larger than the two-photon absorption in dielectrics² since the Keldysh parameter of multiphoton ionization $\gamma \gg 1$.¹⁷ The quiver energy acquired by an electron during an optical oscillation cycle is $\epsilon_{\text{osc}} = 0.12$ eV $\equiv 1393$ K (for a 0.5 nJ pulse). At such temperatures the emission of hot electrons is spectrally broad with maximum at IR spectral region of SU-8

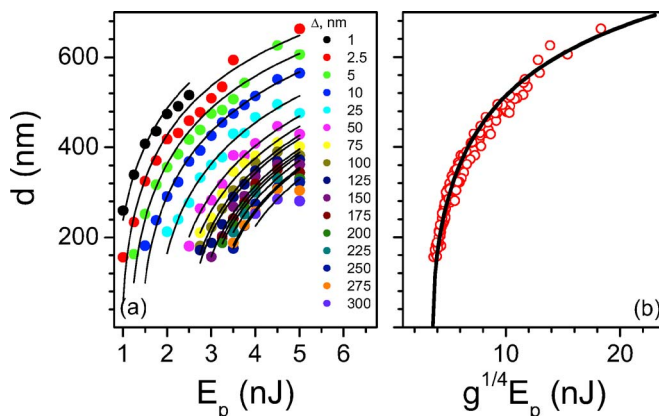


FIG. 3. (a) The dependence of the width of the line d on the pulse energy E_p and pitch Δ (multiplication by a factor of 0.179 should be used to recalculate E_p at focus). The lines are best fits for the Gaussian waist $w_0=360$ nm. (b) The entire experimental data set shown in (a) plotted by Eq. (1) along with the best fit.

absorption as can be directly calculated from Planck's formula [Fig. 1(a)]. The wavelength of emission maximum is given by Wien's law $\lambda_{\max} = \beta/T$, with $\beta = 2.9 \times 10^{-3}$ K m. Absorption by the stretching OH and CH modes at 2.8–3.2 μm and bending modes at 9–10 μm is expected.

The proposed mechanism of thermally enhanced polymerization is different from the accepted view of a nonlinear two-photon absorption dominance in photopolymerization by femtosecond pulses. The narrow range between the photo-damage and exposure threshold for SU-8 at 800 nm differing by only a factor of ~ 2.5 has made it difficult to determine the precise order of the intensity dependence.¹³ The mechanism leading to absorption is conveniently referred to as two photon. It should be noted that the observed scaling can be explained by four-photon absorption ($N=4$) though non-physical at the used of 800 nm wavelength. Indeed, the dependence $d = w_0 \sqrt{(2/N) \ln(E_p/E_{\text{th}})}$,¹⁴ where E_{th} is the threshold of polymerization in terms of pulse energy and w_0 is the waist of the Gaussian pulse, is functionally similar to Eq. (1) at $N=4$. For a pure two-photon polymerization with $N=2$, there would be a $d = w_0 \sqrt{\ln(E_p/E_{\text{th}})}$ dependence expected, which has, however, not fitted the experimental data. The high electron temperature is a distinguished and unique feature of irradiation by ultrashort pulses. Polymerization by picosecond/nanosecond pulses is fundamentally different, since the electron and ion/atom temperatures become stationary during the pulse.

The maximum thermodynamic temperature after energy equilibration between ions and electrons established within several picoseconds after laser pulse is approximately $T = T_e/2$.¹⁶ Thus, for the $T_e = 10^3$ K electron emission the stationary temperature $T = 227$ °C exceeds the thermal polymerization temperature of ~ 167 °C (10 min is required for polymerization¹⁸). The photoinitiator of SU8 is thermally stable at such temperatures.¹¹ The proposed mechanism of thermally enhanced polymerization has been corroborated by (i) the established universal scaling [Eq. (1)] and (ii) observed "optical cure" [Figs. 2(c) and 2(d)].

We further tested the possibility to form 3D photonic crystal structures without postbake, aiming to reduce feature size [Fig. 4(a)]. Optical characterization by typical micro-FTIR (Fourier transform infrared) spectroscopy determined stop-gap wavelength that is tunable to the fiber communication wavelength of 1.33 μm [Fig. 4(b)]. The "optically" cured structures had approximately twice reduced cross sections of polymerized lines.

In conclusion, we have shown that the SU-8 photopolymerization is explainable by absorption of spectrally broad emission of thermally nonequibrated electrons when high-irradiance femtosecond pulses are used for exposure. The temperature rise at the focal region after the pulse was high enough to effectively anneal the focal volume (an optical cure) during direct laser writing. This localized postbake helps further scale down the feature size of laser-fabricated patterns and is expected to be common for the polymeriza-

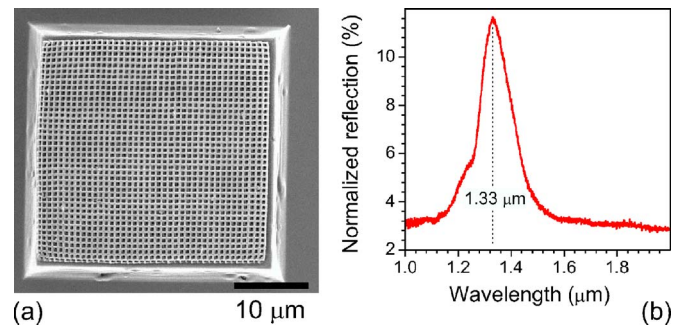


FIG. 4. (a) SEM micrograph of the "optically" cured square spirals of type [001]-diamond:1 (Ref. 9) with $a=0.8$ μm , $L=0.7a$, and $c=1.23a$, $40 \times 40 \times 8$ spiral periods. (b) Reflection spectra of the spiral structure (normalized to gold surface): $a=0.8$ μm , $L=0.7a$, and $c=1.48a$, $40 \times 40 \times 8$. The stop band at 1.33 μm was formed.

tion of resins and resists. The revealed mechanism might be of importance for design of new resist and resin materials, photosensitive glasses, and ceramics, whose photostructuring mechanism is not (or less) dependent on specific photoinitiator when ultrashort high-irradiance laser pulses are used. The spectral width and spectral position of blue wing of emission by nonequibrated electrons can be tuned to the specific wavelength by controlling the irradiance. Three-dimensional structuring of dielectrics is possible by a highly localized three-dimensionally delivered source of thermal emission.

The authors are thankful to V. Mizeikis for critical reading of the manuscript.

- ¹E. N. Glezer, M. Milosavljevic, L. Huang, R. J. Finlay, T.-H. Her, J. P. Callan, and E. Mazur, *Opt. Lett.* **21**, 2023 (1996).
- ²S. Juodkazis, A. V. Rode, E. G. Gamaly, S. Matsuo, and H. Misawa, *Appl. Phys. B: Lasers Opt.* **77**, 361 (2003).
- ³Q. Johnson and A. C. Mitchell, *Phys. Rev. Lett.* **29**, 1369 (1972).
- ⁴S.-D. Mo and W. Y. Ching, *Phys. Rev. B* **57**, 15219 (1998).
- ⁵S. Juodkazis, K. Nishimura, H. Misawa, T. Ebisui, R. Waki, S. Matsuo, and T. Okada, *Adv. Mater. (Weinheim, Ger.)* **18**, 1361 (2006).
- ⁶K. Y. Lee, N. LaBianca, S. A. Rishton, S. Zolgharnain, J. D. Gelorme, J. Shawand, and T. H.-P. Chang, *J. Vac. Sci. Technol. B* **13**, 3012 (1995).
- ⁷J. M. Shaw, J. D. Gelorme, N. C. LaBianca, W. E. Conley, and S. J. Holmes, *IBM J. Res. Dev.* **41**, 81 (1997).
- ⁸M. Deubel, G. von Freymann, M. Wegener, S. Pereira, K. Busch, and C. M. Soukoulis, *Nat. Mater.* **3**, 444 (2004).
- ⁹K. K. Seet, V. Mizeikis, S. Matsuo, S. Juodkazis, and H. Misawa, *Adv. Mater. (Weinheim, Ger.)* **17**, 541 (2005).
- ¹⁰T. Kondo, S. Juodkazis, and H. Misawa, *Appl. Phys. A: Mater. Sci. Process.* **A81**, 1583 (2005).
- ¹¹J. V. Crivello, *Annu. Rev. Mater. Sci.* **13**, 173 (1983).
- ¹²R. C. Rumpf and E. G. Johnson, *J. Opt. Soc. Am. A* **21**, 1703 (2004).
- ¹³G. Witzgall, R. V. E. Yablonovitch, V. Doanand, and B. J. Schwartz, *Opt. Lett.* **23**, 1745 (1998).
- ¹⁴S. Juodkazis, V. Mizeikis, K. K. Seet, M. Miwa, and H. Misawa, *Nanotechnology* **16**, 846 (2005).
- ¹⁵M. Deubel, M. Wegener, A. Kaso, and S. John, *Appl. Phys. Lett.* **85**, 1895 (2004).
- ¹⁶E. G. Gamaly, A. V. Rode, B. L. Davies, and V. T. Tihonchuk, *Phys. Plasmas* **9**, 949 (2002).
- ¹⁷L. V. Keldysh, *Zh. Eksp. Teor. Fiz.* **47**, 1945 (1964) [*Sov. Phys. Solid State* **20**, 1307 (1965)].
- ¹⁸B. H. Ong, X. Yuan, S. Tao, and S. C. Tjin, *Opt. Lett.* **31**, 1367 (2006).